nature photonics

LETTERS

PUBLISHED ONLINE: 20 JULY 2009 | DOI: 10.1038/NPHOTON.2009.117

Silicon nanostructure cloak operating at optical frequencies

Lucas H. Gabrielli[1], Jaime Cardenas[1], Carl B. Poitras[2] and Michal Lipson[3]*

The ability to render objects invisible using a cloak (such that they are not detectable by an external observer) has long been a tantalizing goal[1–6]. Here, we demonstrate a cloak operating in the near infrared at a wavelength of 1,550 nm. The cloak conceals a deformation on a flat reflecting surface, under which an object can be hidden. The device has an area of 225 μm² and hides a region of 1.6 μm². It is composed of nanometre-size silicon structures with spatially varying densities across the cloak. The density variation is defined using transformation optics to define the effective index distribution of the cloak.

The prospect of optical cloaking has recently become a topic of considerable interest. Through the use of transformation optics[7–11], in which a coordinate transformation is applied to Maxwell's equations, several designs for such a device have been created[12–23]. These designs are based on the idea of manipulating the structure of the cloaking medium so that the trajectory of light after interacting with the cloak is the same as that in an empty medium, without the cloak or the object underneath. The external observer is therefore unaware of the presence of the cloak and the object. Such cloaks were recently experimentally demonstrated in the microwave regime using metamaterial structures with feature sizes in the millimetre to centimetre scale[24,25]. Pushing this technology to the optical regime would greatly increase the potential application. However, this requires nanometre control of the cloaking structure.

Here, we demonstrate a cloak in the optical domain operating at 1,550 nm using sub-wavelength scale dielectric structures. We experimentally demonstrate an optical invisibility cloak that hides an object 'under a carpet' with the help of a reflective surface. As outlined in Fig. 1, when an external observer looks at a deformed mirror, the observer detects the deformation in the reflected image (Fig. 1a,b). Following theoretical work by others[11,20], we designed and fabricated a cloaking device at optical frequencies that is capable of reshaping this reflected image and providing the observer with the illusion of looking at a plane mirror (Fig. 1c). Objects could therefore be hidden under such deformations without being detected. A similar device has also been demonstrated that was constructed using a different technique[26].

The cloaking device has a triangular shape with an area of 225 μm², and is composed of a spatially varying density of sub-wavelength 50-nm diameter silicon posts embedded in a SiO_2 medium. The reflective surface consists of a distributed Bragg reflector (DBR) with a deformation that covers the 1.6-μm² cloaked region. The distribution of posts induces a variation of the effective index of refraction across the surface through the relation $\varepsilon_{eff} = \rho_{SiO2}\varepsilon_{SiO2} + \rho_{Si}\varepsilon_{Si}$, where ρ is the volumetric fraction and ε the effective dielectric constant of each material[27]. The DBR consists of alternating regions of SiO_2 and crystalline silicon. The simulated reflectivity for the ten-period DBR used is larger than 0.999. We fabricated the invisibility cloak in a silicon-on-insulator (SOI) wafer. An etching mask, consisting of a 160-nm layer of Dow Corning XR-1541, was patterned by electron-beam lithography, and the 250-nm top silicon layer etched using a standard Cl_2 inductively coupled plasma process. We then clad the device with SiO_2. Scanning electron microscope images of the fabricated device before deposition of the SiO_2 are shown in Fig. 2. A 450-nm-wide silicon waveguide with a tapered end was arranged to terminate at the mid-point of the edge on the y-axis. The waveguide was used to direct light into the device such that all of the input light was incident on the deformation and not on the plane DBR reflector, thereby maximizing the effect of the deformation. Note, however, that the design, based on transformation optics, does not introduce any constraints on the wave fronts applied to the device[20], which means that the cloaking medium operates at all angles of incidence where the reflectance of the DBR is sufficiently high. In Fig. 2b the reduced density of the silicon posts in the low effective index region of the cloak can be observed, as well as some of the silicon sections from which the DBR is composed.

The spatial distribution of the 50-nm-diameter posts, that is, the effective refractive index distribution of the cloak, was determined by defining a transformation of coordinates from the perfect triangle in Fig. 2a to one with a Gaussian-shaped deformation along its hypotenuse (behind which an object could in principle be hidden) for transverse magnetic (TM) polarized fields (with the major component of the electric field perpendicular to the device). To minimize the anisotropy in the medium, the transformation of coordinates was realized by the minimization of the modified Liao functional[20,28,29] with slipping boundary conditions. The resulting effective index distribution has an anisotropy factor of 1.02 with index values ranging from 1.45 to 2.42 between the index of the SiO_2 and that of crystalline silicon, enabling fabrication of the device using standard silicon processes. The complete effective refractive index distribution is shown in Fig. 3. The triangular shape of the device with the deformation along its hypotenuse can be observed. The highest and lowest effective refractive index regions are located around the deformation, and the background index value of the remaining cloaking region is 1.65. The final profile of the cloak contains almost no silicon in the low index regions, whereas in the high index regions it has the largest concentration of posts (see Fig. 2).

We simulated the propagation of light in the device using the finite-difference time-domain (FDTD) method. The results show that, owing to the presence of the cloak, the image of the light incident on the deformation (the region under which an object could be hidden) resembles the image of a wave propagating in a homogeneous medium without the deformation. Figure 4a shows a simulation of light propagating through a homogeneous background index of 1.65 and reflected by the DBR. Figure 4b shows the same simulation when the DBR is deformed, and Fig. 4c shows the simulation of light reflected by the deformed DBR (same as Fig. 4b), but with the deformation now covered by the cloak. By comparing Fig. 4a and b, it can

[1]Nanophotonics Group, School of Electrical and Computer Engineering, 209 Phillips Hall, Cornell University, Ithaca, New York 14853, USA, [2]Nanophotonics Group, School of Electrical and Computer Engineering, 211 Phillips Hall, Cornell University, Ithaca, New York 14853, USA, [3]Nanophotonics Group, School of Electrical and Computer Engineering, 214 Phillips Hall, Cornell University, Ithaca, New York 14853, USA. *e-mail: ml292@cornell.edu

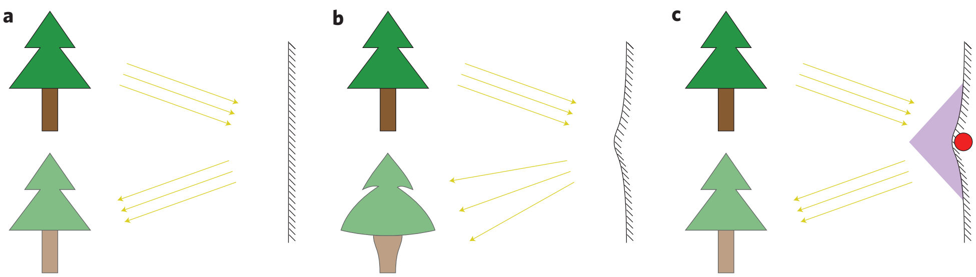

Figure 1 | Cloaking principle of the fabricated device. **a**, A planar mirror forms an image equivalent to the object reflected. **b**,When the mirror is deformed, the image is distorted, allowing an external observer to identify the deformation. **c**, The cloaking device (shaded area in front of the mirror) corrects the distortion in the image, so the observer no longer identifies the deformation in the mirror, nor an object hidden behind the deformation.

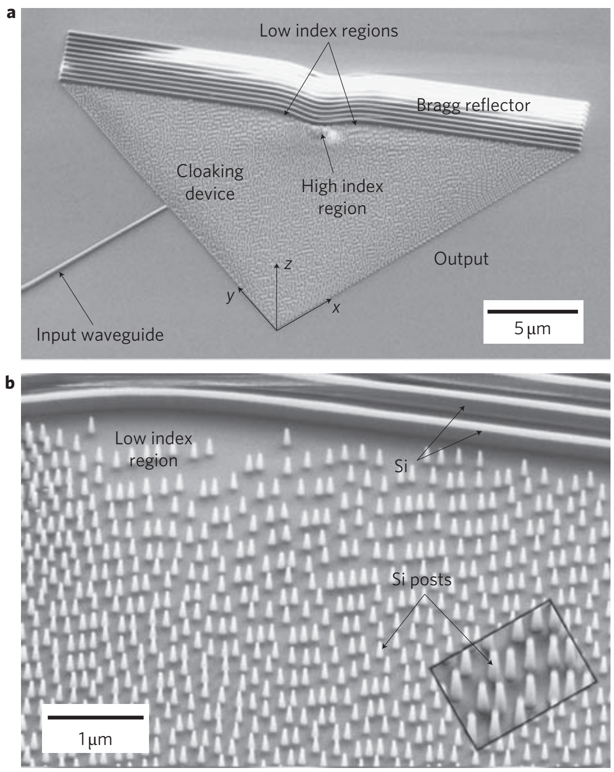

Figure 2 | Scanning electron microscope images of the cloaking device. **a**, Light is coupled to the device through the tapered input waveguide and reflected at the Bragg mirror towards the *xz*-plane. **b**, Silicon posts etched in the SOI wafer with varying density determine the distribution of the effective index of the cloak. Inset: enlarged image of some of the silicon posts.

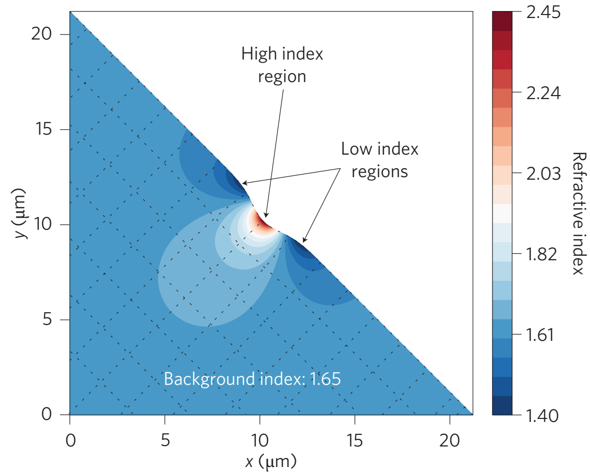

Figure 3 | Two-dimensional spatial effective refractive index distribution of the cloaking device. The effective index values vary between 1.45 and 2.42. The effective background index is 1.65. The dotted lines show the grid transformation.

clearly be seen that the presence of the deformed region can easily be observed in the output image of the device. Figure 4a, the plane DBR in a homogeneous medium, shows a uniform distribution of power along the bottom edge of the device (output), but the deformed mirror (Fig. 4b) presents a power gap as a result of the deformation, creating a power gap at the edge of the device. When the deformation is covered by the cloak (Fig. 4c), this power gap—a signature of the deformation on the DBR—disappears, and the output image resembles that for light propagating through a homogeneous medium and reflected by the plane DBR (Fig. 4a).

We have shown experimentally, using an infrared camera, that the output of the light propagating through the cloak and incident on the deformation in the DBR mirror resembles the image from a plane mirror with no deformation. The device was tested by launching light with a wavelength of 1,550 nm into the waveguide (shown in Fig. 2), then capturing the image at the edge of the device on the *xz*-plane. The infrared camera used for the measurements was set to constant gain, contrast and brightness. The recorded images were filtered using a median filter, with a filter aperture of 15 pixels. Figure 5a shows the image of light reflected from a plane DBR in a homogeneous medium of index 1.65. It can be seen in Fig. 2b that the deformation of the reflector produces the power gap, as predicted from the simulation of the uncloaked deformed mirror. Figure 5c displays the image of light incident on the same deformed DBR, but now covered by the cloaking device. The power gap vanishes, and the image is similar to that reflected from the plane DBR and propagating in a homogeneous medium, as expected.

These results represent the experimental demonstration of an invisibility cloaking device at optical frequencies. The bandwidth and wavelength of operation of the device are limited by the bandwidth of operation of the DBR and, for shorter wavelengths, silicon dispersion. This bandwidth is large (400 nm) around a wavelength of 1,550 nm due to the large index contrast between the silicon and SiO_2. Such a cloak could in principle be reproduced over much larger domains, using techniques such as nanoimprinting, for example, enabling a wide variety of applications in defence, communications and other industries. Note that in this paper we show how the trajectory of light can be manipulated around a region to render it invisible. Using transformation optics in a similar fashion to that used in this paper, one could do the opposite—concentrate light in an area. This could be used for efficiently collecting sunlight in solar energy applications, for example[30].

Received 23 April 2009; accepted 12 June 2009; published online 20 July 2009

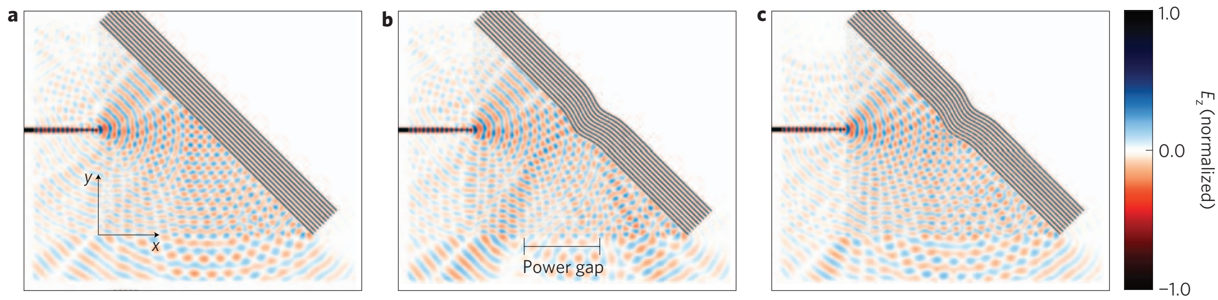

Figure 4 | Simulations of the cloaking device. a, Light at 1,550 nm propagates through a homogeneous background index of 1.65 and is reflected by a plane DBR. **b**, The same arrangement as in **a**, but with the DBR deformed. **c**, The same arrangement as in **b**, but with the deformation covered by the cloak. The deformed mirror (**b**) presents a power gap as a result of the deformation, creating a power gap at the edge of the device. When the deformation is covered by the cloak (**c**), this power gap (a signature of the deformation on the DBR) disappears.

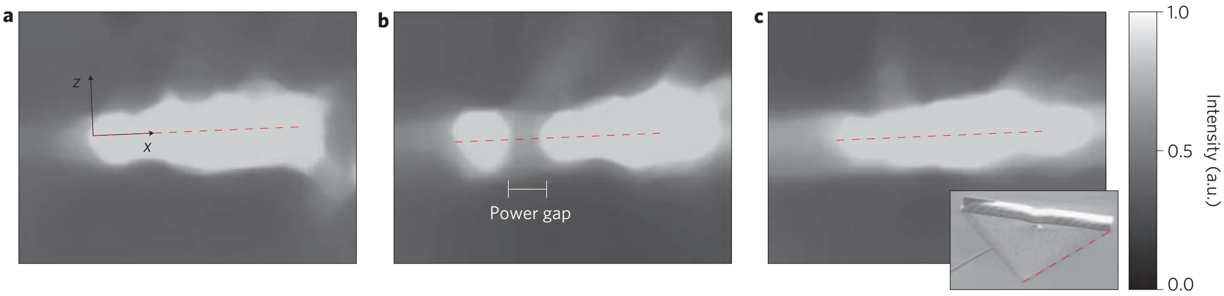

Figure 5 | Output images from the fabricated devices, tested by launching light with a wavelength of 1,550 nm into the waveguide and imaging the edge of the device (dashed lines). These experimental results correspond to the simulation predictions of Fig. 4. **a**, Light reflected from a plane DBR in a homogeneous medium ($n = 1.65$). **b**, Light reflected from a deformed DBR without a cloaking device. **c**, Light reflected from a deformed DBR with the cloaking device, showing that the power gap has vanished, resulting in an image similar to that reflected from the plane DBR (**a**), as expected. Inset: location of the output edge of the device.

References

1. Alú, A. & Engheta, N. Achieving transparency with plasmonic and metamaterial coatings. *Phys. Rev. E* **72,** 016623 (2005).
2. Miller, D. A. B. On perfect cloaking. *Opt. Express* **14,** 12457–12466 (2006).
3. Alú, A. & Engheta, N. Plasmonic materials in transparency and cloaking problems: mechanism, robustness and physical insights. *Opt. Express* **15,** 3318–3332 (2007).
4. Zhao, Y., Argyropoulos, C. & Hao, Y. Full-wave finite-difference time-domain simulation of electromagnetic cloaking structures. *Opt. Express* **16,** 6717–6730 (2008).
5. Weder, R. A rigorous analysis of high-order electromagnetic invisibility cloaks. *J. Phys. A* **41,** 065207 (2008).
6. Weder, R. The boundary conditions for point transformed electromagnetic invisibility cloaks. *J. Phys. A* **41,** 415401 (2008).
7. Ward, A. & Pendry, J. Refraction and geometry in Maxwell's equations. *J. Mod. Opt.* **43,** 773–793 (1996).
8. Leonhardt, U. & Philbin, T. G. General relativity in electrical engineering. *New J. Phys.* **8,** 247 (2006).
9. Pendry, J. B., Schurig, D. & Smith, D. R. Controlling electromagnetic fields. *Science* **312,** 1780–1782 (2006).
10. Kildishev, A. V. & Shalaev, V. M. Engineering space for light via transformation optics. *Opt. Lett.* **33,** 43–45 (2008).
11. Tyc, T. & Leonhardt, U. Transmutation of singularities in optical instruments. *New J. Phys.* **10,** 115038 (2008).
12. Leonhardt, U. Optical conformal mapping. *Science* **312,** 1777–1780 (2006).
13. Cummer, S. A., Popa, B., Schurig, D., Smith, D. R. & Pendry, J. Full-wave simulations of electromagnetic cloaking structures. *Phys. Rev. E* **74,** 036621 (2006).
14. Hendi, A., Henn, J. & Leonhardt, U. Ambiguities in the scattering tomography for central potentials. *Phys. Rev. Lett.* **97,** 073902 (2006).
15. Cai, W., Chettiar, U. K., Kildishev, A. V. & Shalaev, V. M. Optical cloaking with metamaterials. *Nature Photon.* **1,** 224–227 (2007).
16. Ruan, Z., Yan, M., Neff, C. W. & Qiu, M. Ideal cylindrical cloak: perfect but sensitive to tiny perturbations. *Phys. Rev. Lett.* **99,** 113903 (2007).
17. Chen, H., Wu, B., Zhang, B. & Kong, J. A. Electromagnetic wave interactions with a metamaterial cloak. *Phys. Rev. Lett.* **99,** 063903 (2007).
18. Huang, Y., Feng, Y. & Jiang, T. Electromagnetic cloaking by layered structure of homogeneous isotropic materials. *Opt. Express* **15,** 11133–11141 (2007).
19. Silveirinha, M. G., Alu, A. & Engheta, N. Parallel-plate metamaterials for cloaking structures. *Phys. Rev. E* **75,** 036603 (2007).
20. Li, J. & Pendry, J. B. Hiding under the carpet: a new strategy for cloaking. *Phys. Rev. Lett.* **101,** 203901 (2008).
21. Alú, A. & Engheta, N. Multifrequency optical invisibility cloak with layered plasmonic shells. *Phys. Rev. Lett.* **100,** 113901 (2008).
22. Jiang, W. X. *et al.* Analytical design of conformally invisible cloaks for arbitrarily shaped objects. *Phys. Rev. E* **77,** 066607 (2008).
23. Leonhardt, U. & Tyc, T. Broadband invisibility by non-Euclidean cloaking. *Science* **323,** 110–112 (2009).
24. Schurig, D. *et al.* Metamaterial electromagnetic cloak at microwave frequencies. *Science* **314,** 977–980 (2006).
25. Liu, R. *et al.* Broadband ground-plane cloak. *Science* **323,** 366–369 (2009).
26. Valentine, J., Li, J., Zentgraf, T., Bartal, G. & Zhang, X. An optical cloak made of dielectrics. *Nature Mater.* **8,** 569–571 (2009).
27. Nakamura, T., Shimizu, M., Kimura, H. & Sato, R. Effective permittivity of amorphous mixed materials. *Electron. Commun. Jpn. 1* **88,** 1–9 (2005).
28. Knupp, P. M. & Steinberg, S. *Fundamentals of Grid Generation* (CRC Press, 1993).
29. Thompson, J. F., Soni, B. K. & Weatherill, N. P. *Handbook of Grid Generation* (CRC Press, 1998).
30. Shalaev, V. M. Physics: transforming light. *Science* **322,** 384–386 (2008).

Acknowledgements

The authors would like to acknowledge the support of Cornell's Center for Nanoscale Systems (CNS), funded by the National Science Foundation. This work was performed in part at the Cornell Nanoscale Facility, a member of the National Nanotechnology Infrastructure Network, which is supported by the National Science Foundation.

Author contributions

L.H.G. designed and simulated the devices. L.H.G. and J.C. carried out the fabrication of the samples. L.H.G. and C.B.P. conducted the experiments. L.H.G., C.B.P. and M.L. designed the experiments and discussed their results and implications.

Additional information

Reprints and permission information is available online at http://npg.nature.com/reprintsandpermissions/. Correspondence and requests for materials should be addressed to M.L.